

Constrained equitable 3-cuttings

Sergei Bespamyatnikh¹ and David Kirkpatrick²

¹ Department of Computer Science, University of Texas at Dallas,
Box 830688, Richardson, TX 75083, USA

`besp@utdallas.edu`

² Department of Computer Science, University of British Columbia,
201-2366 Main Mall, Vancouver, B.C., V6T 1Z4, Canada

`kirk@cs.ubc.ca`

Abstract. We investigate equitable 3-cuttings of two mass distributions in the plane (partitions of the plane into 3 sectors with a common apex such that each sector contains 1/3 of each mass). We prove the existence of a continuum of equitable 3-cuttings that satisfy some closure property. This permits us to generalize earlier results on both convex and non-convex equitable 3-cuttings with additional constraints.

1 Introduction

This paper continues recent results [2, 4, 8, 13, 9] generalizing the Ham Sandwich Theorem for the plane. The planar case of the discrete Ham Sandwich Theorem [16] states that, for finite sets of red and blue points in the plane, there exists a line dividing both red and blue points into sets of equal size. The Ham Sandwich problem is well studied from an algorithmic point of view [1, 5–7, 10–12, 14, 17]. An optimal algorithm of Lo et al. [11] finds a Ham Sandwich cut in linear time. Kaneko and Kano [9] considered balanced partitions of two sets in the plane. They conjectured that, for any gn red and gm blue points ($g, n, m > 0$ are integers) in the plane in general position, there are g disjoint convex polygons with n red and m blue points in each of them. The conjecture of Kaneko and Kano has been independently proven by Ito et al. [8] (the case $g = 3$), Sakai [13] and Bespamyatnikh et al. [4]. Only [4] considered algorithmic issues related to this conjecture. In particular they showed that a balanced partition can be constructed in $O(N^{4/3} \log^3 N \log g)$ time, where $N = n + m$.

For the case $g = 3$, it is shown in [4] that it suffices to consider 3-cuttings, partitions of the plane into three wedges with a common apex. More specifically, either the points of R and B admit a *T-shaped* equitable 3-cutting, formed by two successive 2-cuttings, or there is a *Y-shaped* convex equitable 3-cutting constrained to have one (reference) ray directed vertically downward (see Figure 1). (From an algorithmic perspective the second case presents the main challenge; the first reduces to the standard Ham Sandwich construction.) Bárány and Matoušek [2] establish a number of results concerning the existence (and non-existence) of (not necessarily convex) 3-cuttings with specific triples that define (not necessarily equal) portions of the points in the wedges. In this paper

we restrict our attention to the case $g = 3$ (with the equal portions $(\frac{1}{3}, \frac{1}{3}, \frac{1}{3})$) but admit arbitrary directions of the reference ray. A central objective of our investigation is to provide a characterization all such 3-cuttings that partition one color (red) equitably. We show that these can be represented using 3-colored arrangements in the plane. Assuming that the masses do not admit a T-shaped equitable 3-cutting, the space of possible convex 3-cuttings with fixed direction of the reference ray is neatly captured by what we call a *triangle diagram* that is of interest in its own right. We prove the existence of a special 3-cutting in a perfect triangle diagram that we call a *centroid*.

We establish an invariant of the triangle diagram under rotation of the reference direction. We use it to prove the Centroid Theorem which allows a direct proof of the existence of an equitable 3-cutting with a variety of reasonable constraints (in place of a fixed direction of the reference ray).

Theorem 1 (Constrained convex 3-cutting). *For any two Borel probability measures either there exists a T-shaped convex equitable 3-cutting or there is an equitable 3-cutting satisfying any one of the following constraints:*

- (a) *One of the rays passes through any specific point, not necessarily in the plane. (The special case of the point $(0, -\infty)$ corresponds to the the constraint of the starting ray going directly down).*
- (b) *The angle of one of the wedges is $2\pi/3$.*
- (c) *One of the wedges has weight $1/3$ of a third mass.*
- (d) *Two rays are symmetric with respect to the line through the third ray.*
- (e) *The angles of the wedges form an arithmetic progression.*

A T-shaped 3-cutting or a 3-cutting satisfying the condition 3 of Theorem 1 generates $(1/3, 2/3)$ 2-fan partition of three masses which was first shown in [2]. For general (not necessarily convex) 3-cuttings we prove the existence of equitable 3-cutting without a condition of T-shaped cutting.

Theorem 2 (Constrained 3-cutting). *For any two Borel probability measures there exists an equitable 3-cutting satisfying any one of the constraints (a)-(e) from Theorem 1.*

Theorem 2 is a strengthening of a result by Bárány and Matoušek [2] that states the existence of unconstrained equitable 3-cutting.

We also mention a recent paper by Vrećica and Živaljević [15] on conical equipartitions and a paper by Bárány and Matoušek [3] on equipartitioning two masses by 4-fans.

2 Preliminaries

Let P_R be a set of n red points in the plane and let P_B be a set of m blue points in the plane such that all the points are in general position (the points are distinct and no three points are collinear). A *3-cutting* is a partition of the plane into 3 wedges W_1, W_2 and W_3 by 3 rays with a common point that is called the *apex*

of the 3-cutting. A 3-cutting is *convex* if its wedges are convex. A 3-cutting is *equitable* if each wedge (as open set) contains at most $n/3$ of red points and at most $m/3$ blue points. One of the rays is defined as the *reference ray*. We call the wedges adjacent to the reference ray the *left* and *right* wedges. The remaining wedge is the *upper* wedge. The rays different from the reference ray are called *left*, *right*. (Note that at most one of the wedges can be non-convex.)

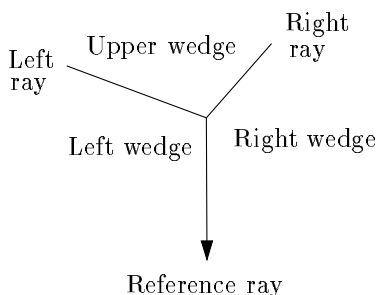


Fig. 1. The notation of a 3-cutting.

Canonical 3-cutting. Let μ be a mass in the plane. For a point p and a direction d , we define a *canonical 3-cutting* as follows. The reference ray emanates from p in the direction d . The left ray maximizes the angle of the left wedge W_1 such that the weight of the interior of W_1 is at most $1/3$. The right ray maximizes the angle of the right wedge W_3 such that the weight of the interior of W_3 is at most $1/3$. If μ' is another mass in the plane we define a *sign* $s_i(\mu, \mu')$, $i = 1, 2, 3$ to be the μ' -weight of the wedge W_i minus $1/3$.

Pseudo-discrete masses. A *mass* μ in the plane is defined by a Borel probability measure $\mu : \mathbb{R}^2 \rightarrow \mathbb{R}$. A *discrete mass* $\mu(P)$ induced by a set of points P is defined so that a weight of a region R is the number of points in $P \cap R$ divided by the number of points in P . It suffices to prove Theorems 1 and 2 for discrete masses, using a reduction from continuous to discrete mass distributions described in [4]. We would like the masses to behave like continuous ones in the sense that every canonical 3-cutting changes continuously when its apex moves on the plane. We introduce *pseudo-discrete masses* that are generated by finite sets P_R and P_B of red and blue points, and whose canonical 3-cuttings are continuous. We put a disk $D(p)$ of sufficiently small radius at every red and blue point $p \in P_B \cup P_R$. We draw two concentric circles C_R and C_B of a large radius such that all disks $D(p)$ are inside both C_R and C_B . We assign a small portion of red mass to C_R and a small portion of blue mass to C_B . We assume that these masses are distributed uniformly although one can use non-uniform distributions. The remaining red and blue masses are distributed among disks so that each red (resp. blue) disk is assigned the same portion of the remaining red (resp. blue) mass. We assume that the distributions of masses in the disks

are defined by centrally symmetric polynomial functions. The pseudo-discrete masses capture discrete masses (if the weights of the circles C_R and C_B and the disk radii tend to 0) and allow us to achieve properties useful for proving Theorems 1 and 2.

Hereafter we assume that masses are pseudo-discrete. Let $s_i(p)$, $i = 1, 2, 3$ be the sign of the canonical 3-cutting with apex at p with respect to the pseudo-discrete masses. We partition the plane according to the signs $s_i(p)$, $i = 1, 2, 3$. There 27 possible combinations of signs (each sign s_i , $i = 1, 2, 3$ can be either < 0 or $= 0$ or > 0). We call this partition a *sign partition* of the plane.

Sign Components. Red and blue point sets P_R and P_B admit pseudo-discrete masses such that there are finitely many connected components in the sign partition and each component has dimension corresponding to constraints³. For example, a component constrained as $s_1(p) = s_2(p) = s_3(p) = 0$ is a point (dimension 0), a component with constraints $s_1(p) = 0, s_2(p) < 0, s_3(p) > 0$ is a curve (dimension 1) and a component with constraints $s_1(p) < 0, s_2(p) > 0, s_3(p) > 0$ is a two-dimensional region bounded by a curve.

3 Triangle diagram

In this section we introduce a notion of *triangle diagram* that allows us to characterize all equitable 3-cuttings with vertical reference ray. A study of triangle diagrams may be of independent interest.

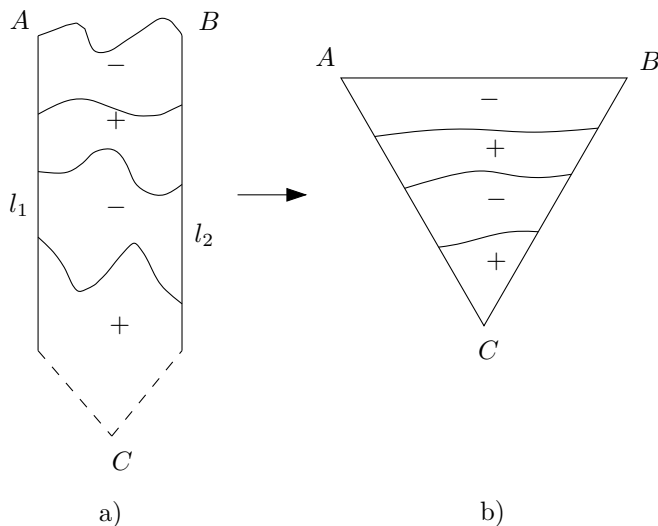


Fig. 2. The levels of s_2 .

³ We can show this property using polynomial distributions of constant degree.

We consider only convex 3-cuttings in this section. We assume that the masses satisfy a *sign property*: any halfplane with red weight $1/3$ has blue weight less than $1/3$. The sign property eliminates the case of T-shaped 3-cuttings in Theorem 1.

There are two vertical lines l_1, l_2 cutting the red mass into 3 pieces of equal weight $1/3$. One can show that the locus of apexes of convex red 3-cuttings with one ray going down is a region R sandwiched by these lines from left and right side. The upper boundary of R is defined by a x -monotone curve connecting the left and right sides, say points A and B , see Fig. 2 a). Two parallel lines l_1 and l_2 “meet” at point C with $y = -\infty$. We represent R as a regular triangle, see Fig. 2 b).

The upper wedge of red 3-cuttings with apexes on the curve AB has angle 2π . The sign property implies that the blue weight of the upper wedge is less than $1/3$. In other words $s_2(p) < 0$ for all points p on the curve AB . Note that $s_2(p)$ becomes positive if p goes far enough down in the region R because the left and right rays of red 3-cutting go to the left and right sides of R . Let $k_2(p)$ be the smallest number of times the sign $s_2()$ changes along a path from a point p to AB . Let Ξ be the set of paths from C to AB with exactly $k_2(C)$ changes of the sign $s_2()$ along the path. We define i -th s_2 -level, $1 \leq i \leq k_2(C)$ as the locus of points p from the paths $\xi \in \Xi$ such that $k_2(p) = i - 1$ and $s_2(p) = 0$.

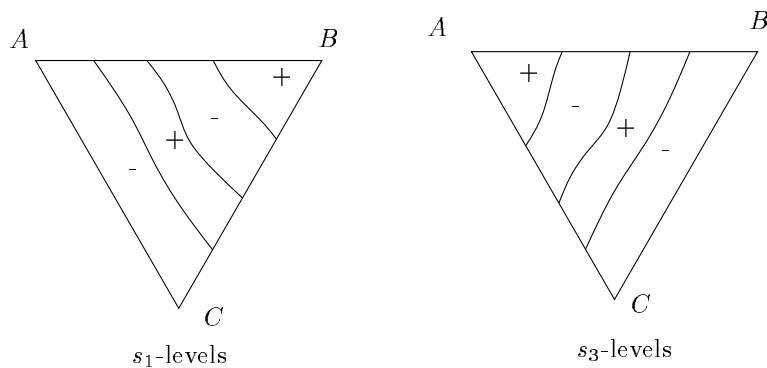


Fig. 3. The levels of s_1 and s_3 .

The sign $s_1()$ is negative for the points in the side AC and is positive at B . We define s_1 -levels similarly to s_2 -levels. s_1 -levels connect the sides AB and BC , see Fig. 3 a). Similarly we define s_3 -levels using signs $s_3()$, see Fig. 3 b). The arrangement of s_1 -, s_2 - and s_3 -levels is a *triangle diagram*. We are interested in topological properties of triangle diagrams so the mapping from the plane to the triangle diagram does not need to be uniquely defined.

Lemma 1. *For every $i = 1, 2, 3$, the s_i -levels are disjoint curves.*

We color s_1 -, s_2 - and s_3 -levels in red, blue and green colors respectively producing a diagram. The levels satisfy the following properties.

Oddness Property. The number of levels of each color is odd.

Intersection Property. If two levels of different colors intersect at point p then a level of the third color intersects p .

The intersection property follows from the fact that, for every point p

$$s_1(p) + s_2(p) + s_3(p) = 0 \quad (1)$$

(if, say $s_1(p) = s_2(p) = 0$, then $s_3(p) = 0$). Do the above properties capture sufficient conditions of a triangle diagram? The answer is “no” and Fig. 4 illustrates an unrealizable diagram. It is unrealizable diagram because the middle triangle has all positive signs contradicting with Equation 1. A new condition can be expressed in the following way.

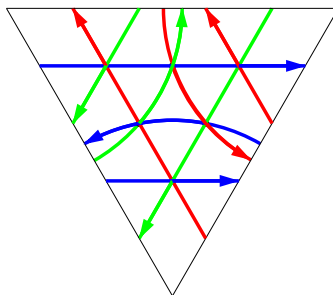


Fig. 4. Impossible diagram.

We orient levels such that the left side of an oriented level has negative sign s_i corresponding to the level. It is easy to show that the levels intersecting in the same point have *alternating directions* in-out-in-out-in-out, see Fig. 5. Note that the vertices of the middle triangle in Fig. 4 do not have alternating directions of the levels.

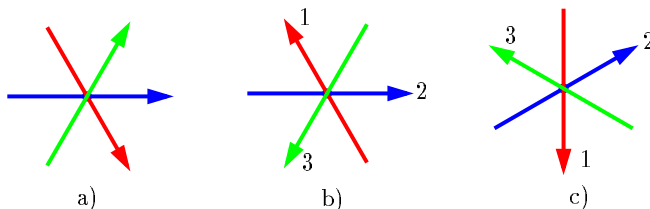


Fig. 5. Orientations of intersecting levels. a) Infeasible orientations. b), c) Feasible orientations.

We define a *triangle diagram* as a digram satisfying the oddness property, the intersection property and the alternating directions. Simple examples of triangle diagrams are shown in Fig. 6.⁴

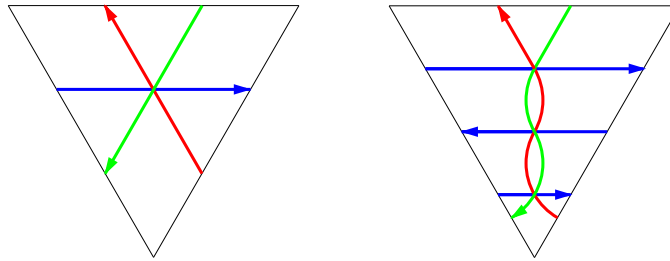


Fig. 6. Simple triangle diagrams.

The triangle diagrams satisfy a chessboard property, i.e. the faces can be colored in two colors, black and white, such that any two faces sharing an edge have different colors.

The triangle diagram changes under rotation of the initial direction of the reference ray. We say that a triangle diagram is *perfect* if it is topologically invariant under rotation, see Fig. 7. The perfect diagrams in Fig. 7 have unique central vertices that play key role in rotating 3-cuttings. Each 3-cutting appears 3 times under rotation. An equitable 3-cutting is a *centroid* if its corresponding 3-cuttings are connected under rotation. Our main result in the triangle diagrams is the existence of a centroid in a perfect diagram⁵.

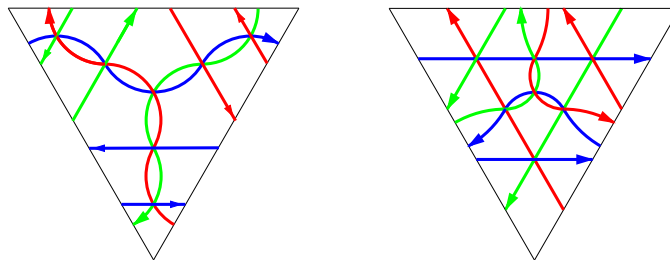


Fig. 7. Perfect triangle diagrams.

⁴ Colored pictures of triangle diagrams are available in the website <http://www.utd.edu/~besp/3diagram>.

⁵ Due to lack of space some proofs will be in full paper.

Theorem 3 (Centroid). *Each perfect triangle diagram has a unique centroid vertex.*

4 General (not necessarily convex) 3-cuttings

In this section we consider only 3-cuttings with the reference ray directed down. For every point in the plane there is a unique red 3-cutting with reference ray directed down. This red 3-cutting is not necessarily convex but, of course, at most one of its wedges can be non-convex. We also allow 3-cuttings whose apexes are at infinity, see Fig. 8.

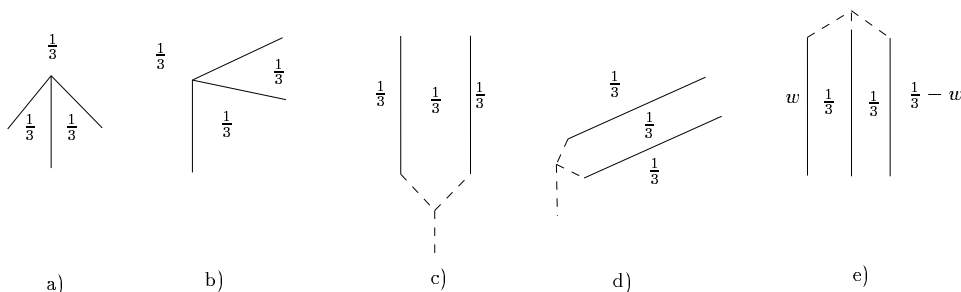


Fig. 8. a), b) non-convex 3-cuttings. c), d) e) converging 3-cuttings.

Consider the arrangement \mathcal{A} defined by the levels on the entire plane. Let l_1 and l_2 be the vertical lines partitioning the red mass into 3 parts of equal weight $1/3$. Let a , b and c be the blue weights of corresponding parts. The boundary of the plane can be viewed as a “shield” ABCDEA, see Fig. 9 a), where B and C are top points of the lines l_1 and l_2 ; E is a bottom point of l_1 and l_2 ; A and D represent the top line points going to the left and to the right respectively. Note that A and D represent the same 3-cuttings. The 3-cuttings with apexes at A , B , C , D and E have blue weights a , b and c as depicted in Fig. 9 a). Let S (shield) denote the space of all 3-cuttings with glued points A and D .

Internal vertices. Each internal vertex has degree 6 and is formed by 3 levels. There are two types of the internal vertices of the arrangement \mathcal{A} , see Fig. 5 b) and c). We label a vertex as “+” if the outgoing levels form the sequence 123 in clockwise order, see Fig. 5 c). Otherwise it has label “-”.

Edges. The internal vertices split level curves into *internal* and *external* edges. An internal edge is a part of level curve between two internal vertices. External edges remain when internal edges are removed from levels. By the alternating directions property the endpoints of an internal edge are internal vertices with opposite labels.

Faces. The faces are labeled by labels that are shown in Fig. 9 b). The face labeling satisfies the transition property that two faces separated by an edge have two consecutive labels on the label diagram.

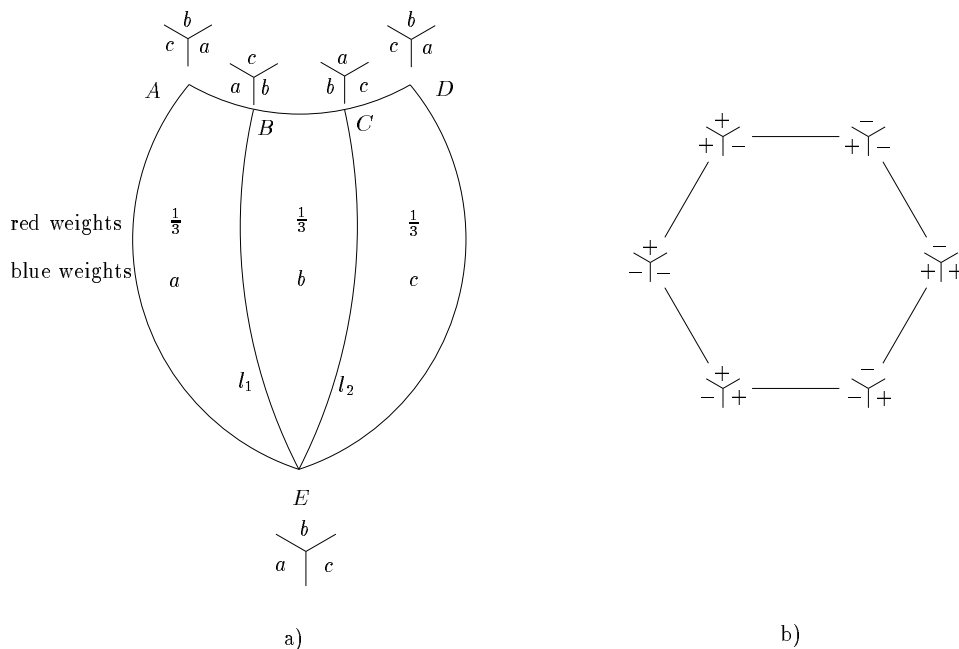


Fig. 9. a) The boundary of the plane. b) The label diagram.

Let v^+, v^- denote the number of the internal vertices labeled by “+” and “-” respectively. Let b^+, b^- denote the number of the external edges adjacent to internal vertices with corresponding labels.

Theorem 4. *Let t be the number of turns of the closed path on label diagram 9 b) when one walks on the boundary of \mathcal{A} in clockwise order. Then*

$$v^+ - v^- = \frac{b^+ - b^-}{6} = t \tag{2}$$

and $t \equiv -1 \pmod{3}$.

Proof. Let e be the number of edges in the arrangement \mathcal{A} that are incident to an internal vertex. These edges can be counted using positive endpoints. Each internal vertex labeled “+” participates in six edges and remaining edges are external. Similar counting can be done for negative vertices. Hence

$$e = 6v^+ + b^- = 6v^- + b^+$$

and the first equality of (2) follows.

To prove the second equality of the equation (2) we consider the clockwise order closed path on the boundary \mathcal{A} . Suppose we cross the external edge e incident to the internal vertex p labeled “+”. The face labels around p are shown

in Fig. 10 a). There are six faces and their labels have the same order as the one in the label diagram, see Fig. 9 b). Hence the label transition is the rotation on clockwise angle $\pi/3$ in label diagram.

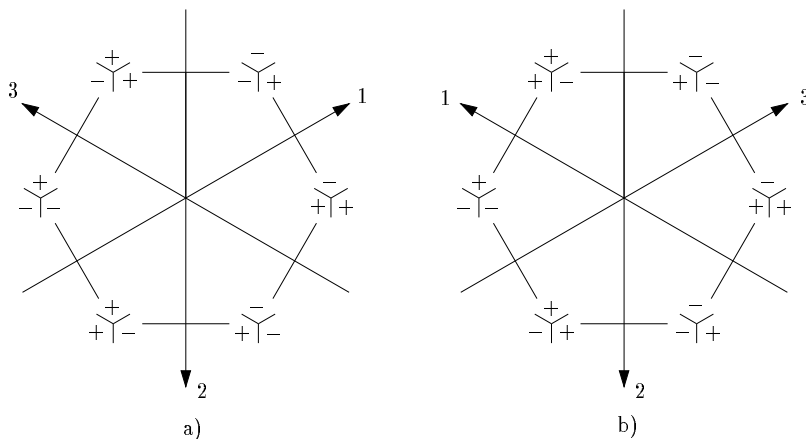


Fig. 10. The vertex labels a) “+” b) “-”.

Suppose we cross the external edge e incident to the internal vertex p labeled “-”. The face labels around p are shown in Fig. 10 b). The order of labels is opposite to the one in the label diagram. Hence the label transition is the rotation on counterclockwise angle $\pi/3$ in label diagram. It follows that each edge counted in b^+ participates as $1/6$ of clockwise turn in the label diagram. The contribution of an edge counted in b^- is $-1/6$. It implies $(b^+ - b^-)/6 = t$. Note that edges whose endpoints are on the boundary contribute 0 into t .

There is a bijection between the boundaries EA and DE . Each 3-cutting corresponding to a point in EA is defined by 2 parallel non-vertical lines equipartitioning the red mass, see Fig. 8 d). Consider such a pair of lines. Let $a + 1/3$, $b + 1/3$ and $c + 1/3$ be the blue weights of the upper halfplane, the middle slab and the lower halfplane respectively. The triple (s_1, s_2, s_3) of signs for the point in EA is (a, b, c) . These lines define 3-cutting for a point in the left boundary ED and the corresponding sign triple is (c, b, a) .

Consider the motion through an external edge in EA . Let $(a, b, c) - (a', b', c')$ be the label transition. The corresponding label transition in DE is $(c, b, a) - (c', b', a')$. These transitions are opposite in the label diagrams and they are cancelled in total rotation of angle 0 along DEA .

Consider the motion along the boundary $ABCD$. Each 3-cutting corresponding to a point in AB is defined by three parallel vertical lines equipartitioning the red mass, see Fig. 8 e). Each such three lines define three 3-cuttings with one of the lines specifying the reference ray. The labels of these 3-cuttings form regular triangle in the label diagram. Hence the rotation on the label diagram

defined by walk along AB is the same as ones along BC and CD . The labels in A , B and C also form a regular triangle in the label diagram. Suppose r is the label rotation along AB in terms of clockwise turns (the clockwise turn is 1). Hence $r = t' - 1/3$ where t' is integer. It follows $t = 3(t' - 1/3) \equiv -1 \pmod{3}$ and we are done.

Theorem 5 (Existence of general 3-cutting). *For any red and blue masses in the plane and for any direction d there is an equitable (not necessarily convex) 3-cutting with one ray in the direction d .*

Proof. We can assume that d is the downward direction. Theorem 4 establishes property that $v^+ - v^- \not\equiv 0 \pmod{3}$. It implies that $v^+ - v^-$ is non-zero and there is at least one internal vertex in \mathcal{A} . This vertex is an apex of an equitable 3-cutting with one ray going down. The theorem follows.

5 Centroid Theorems

In this section we consider 3-cuttings under rotation of the reference ray. Theorem 4 establishes property of $v^+ - v^-$. We extend Theorem 4 and prove that $v^+ - v^-$ is invariant under rotation.

Using Theorem 4 we prove a property of the centroid under rotation. Consider an arrangement \mathcal{A}' in the space $S' = S \times S^1$ induced by \mathcal{A} where S^1 is the space of rotations (the space of reference ray directions). A point (p, α) in the space S' determines the red 3-cutting $c(p, \alpha)$ in the plane with apex p and the reference ray with slope α . Let $\alpha_1(p, \alpha)$ and $\alpha_2(p, \alpha)$ denote the slopes of the left and right rays of the 3-cutting $c(p, \alpha)$. There is the map $\gamma : S' \rightarrow S'$ defined by $\gamma(p, \alpha) = (p, \alpha_1(p, \alpha))$. In other words each 3-cutting appears 3 times under rotation. So we call the map γ a *rotation*.

We prove⁶ the existence of a centroid for pseudo-discrete masses. It can be extended to Borel probability measures, see discussion in [2, 4].

Theorem 6 (Centroid of general 3-cuttings). *For any two Borel probability measures in \mathbb{R}^2 there is a centroid.*

It is straightforward to verify using Theorem 6 that each constraint of Theorem 2 can satisfied by a 3-cutting. Theorem 6 also can be used to prove the following generalization of Theorem 3. We call a centroid *convex* if all its 3-cuttings are convex.

Theorem 7 (Convex 3-cuttings). *For two Borel probability measures with the sign property there is a unique convex centroid.*

Theorem 1 follows from Theorem 7.

⁶ in full version of the paper.

References

1. I. Bárány. Geometric and combinatorial applications of Borsuk's theorem. In J. Pach, editor, *New Trends in Discrete and Computational Geometry*, volume 10 of *Algorithms and Combinatorics*, pp. 235–249. Springer-Verlag, 1993.
2. I. Bárány and J. Matoušek. Simultaneous partitions of measures by k -fans. *Discrete Comput. Geom.*, 25(3):317–334, 2001.
3. I. Bárány and J. Matoušek. Equipartition of two measures by a 4-fan. *Discrete Comput. Geom.*, 27(3):293–301, 2002.
4. S. Bespamyatnikh, D. Kirkpatrick, and J. Snoeyink. Generalizing ham sandwich cuts to equitable subdivisions. *Discrete Comput. Geom.*, 24(4):605–622, 2000.
5. M. Díaz and J. O'Rourke. Ham-sandwich sectioning of polygons. In *Proc. 2nd Canad. Conf. Comput. Geom.*, pp. 282–286, 1990.
6. D. P. Dobkin and H. Edelsbrunner. Ham-sandwich theorems applied to intersection problems. In *Proc. 10th Internat. Workshop Graph-Theoret. Concepts Comput. Sci.*, pp. 88–99, 1984.
7. H. Edelsbrunner and R. Waupotitsch. Computing a ham-sandwich cut in two dimensions. *J. Symbolic Comput.*, 2:171–178, 1986.
8. H. Ito, H. Uehara, and M. Yokoyama. 2-dimension ham sandwich theorem for partitioning into three convex pieces. In *Proc. Japan Conf. Discrete Comput. Geom.'98*, volume 1763 of *Lecture Notes Comput. Sci.*, pp. 129–157. Springer-Verlag, 2000.
9. A. Kaneko and M. Kano. Balanced partitions of two sets of points in the plane. *Comput. Geom. Theory Appl.*, 13:253–261, 1999.
10. C.-Y. Lo, J. Matoušek, and W. Steiger. Ham-sandwich cuts in \mathbb{R}^d . In *Proc. 24th Annu. ACM Sympos. Theory Comput.*, pp. 539–545, 1992.
11. C.-Y. Lo, J. Matoušek, and W. L. Steiger. Algorithms for ham-sandwich cuts. *Discrete Comput. Geom.*, 11:433–452, 1994.
12. C.-Y. Lo and W. Steiger. An optimal-time algorithm for ham-sandwich cuts in the plane. In *Proc. 2nd Canad. Conf. Comput. Geom.*, pp. 5–9, 1990.
13. T. Sakai. Balanced convex partitions of measures in \mathbb{R}^2 . *Graphs and Combinatorics*, 18(1):169–192, 2002.
14. W. Steiger. Algorithms for ham sandwich cuts. In *Proc. 5th Canad. Conf. Comput. Geom.*, p. 48, 1993.
15. S. T. Vrećica and R. T. Živaljević. Conical equipartitions of mass distributions. *Discrete Comput. Geom.*, 25(3):335–350, 2001.
16. R. T. Živaljević. Topological methods. In J. E. Goodman and J. O'Rourke, editors, *Handbook of Discrete and Computational Geometry*, chapter 11, pp. 209–224. CRC Press LLC, Boca Raton, FL, 1997.
17. R. T. Živaljević and S. T. Vrećica. An extension of the ham sandwich theorem. *Bull. London Math. Soc.*, 22:183–186, 1990.